

to the superspace. Such localized configurations could then help our understanding of quark confinement¹⁰ and hadronic matter (bags). These solutions could also shed light on the bubble formation in early universe.

It is a pleasure to thank R. Jackiw for suggestions and discussions, and A. Kupiainen and A. Luther for discussions. Part of this work was completed at Helsinki University of Technology and I thank E. Byckling and K. Kajantie for their hospitality. This work was supported in part by the U. S. Department of Energy under Contract No. DE-ACO2-76ERO3069.

Note added.—After completion of this manuscript I learned that J. Cardy (University of Washington, Seattle) has also found finite-energy solitons and arrived at similar conclusions.

^(a)Present address.

¹G. Grinstein, Phys. Rev. Lett. **37**, 944 (1976); A. Aharony, Y. Imry, and S. K. Ma, Phys. Rev. Lett. **37**, 1364 (1976); A. Young, J. Phys. C **10**, L257 (1977).

²G. Parisi and N. Sourlas, Phys. Rev. Lett. **43**, 744 (1979).

³T. Banks, Tel Aviv University Report No. 1020-82, 1982 (to be published).

⁴B. McClain, A. Niemi, and C. Taylor, Ann. Phys.

(N.Y.) **140**, 232 (1982).

⁵A. Niemi and L. C. R. Wijewardhana, Ann. Phys. (N.Y.) **140**, 247 (1982).

⁶B. McClain, A. Niemi, C. Taylor, and L. C. R. Wijewardhana, Phys. Rev. Lett. **49**, 252 (1982), and Massachusetts Institute of Technology Center for Theoretical Physics Report No. 996, 1982 (to be published).

⁷A. Niemi and L. C. R. Wijewardhana, to be published.

⁸E. Pytte, Y. Imry, and D. Mukamel, Phys. Rev. Lett. **46**, 1172 (1981); H. S. Kogon and D. J. Wallace, J. Phys. A **14**, L527 (1981).

⁹Y. Imry and S. K. Ma, Phys. Rev. Lett. **35**, 1399 (1975); G. Grinstein and S. K. Ma, Phys. Rev. Lett. **49**, 685 (1982).

¹⁰P. Olesen, Nucl. Phys. **B200**, 381 (1982); A. Kupiainen and A. Niemi, Massachusetts Institute of Technology Center for Theoretical Physics Report No. 1025, 1982 (to be published).

¹¹A. Kupiainen and A. Niemi, unpublished.

¹²H. Yoshizawa, R. A. Cowley, G. Shirane, R. J. Birgeneau, H. J. Guggenheim, and H. Ikeda, Phys. Rev. Lett. **48**, 438 (1982).

¹³See, e.g., S. Coleman, in *The Whys of Subnuclear Physics*, edited by A. Zichichi (Academic, New York, 1978).

¹⁴C. Callan, R. Dashen, and D. Gross, Phys. Rev. D **17**, 2717 (1978), and **19**, 1826 (1979), and **20**, 3279 (1979).

Influence of Collective Surface Motion on the Threshold Behavior of Nuclear Fusion

W. Reisdorf, F. P. Hessberger, K. D. Hildenbrand, S. Hofmann, G. Münzenberg,
K.-H. Schmidt, J. H. R. Schneider, W. F. W. Schneider,
K. Sümmerer, and G. Wirth

Gesellschaft für Schwerionenforschung, D-6100 Darmstadt, Germany

and

J. V. Kratz and K. Schlitt

Institut für Kernchemie, Universität Mainz, Federal Republic of Germany

(Received 16 August 1982)

Fusion excitation functions for the systems $^{40}\text{Ar}+^{112,116,122}\text{Sn}$ and $^{40}\text{Ar}+^{144,148,154}\text{Sm}$ have been determined, covering cross sections ranging from several hundred millibarns down to the microbarn level. The data are interpreted with a fusion model that includes fluctuations of the barrier with an amplitude that is shown to be correlated with the collective surface properties of the nuclei. There is no need to assume an additional enhanced tunneling process.

PACS numbers: 25.70.Bc, 21.60.Ev, 25.70.Fg

Mechanisms influencing the fusion of massive nuclei at energies in the threshold region are still insufficiently understood. Vaz, Alexander, and Satchler¹ have pointed out that for energies

below the experimentally determined *s*-wave barrier, the observed cross sections were systematically larger than expected from conventional one-dimensional barrier penetration mod-

els. A scaling of this observation with the mean reduced curvature radii of the dinuclear system at "contact," i.e., with the size of the opposing nuclear surfaces, was suggested by Jahnke *et al.*² A global effect, such as the formation of a "neck" between the nuclei, was proposed,^{1,2} that could introduce a new degree of freedom allowing by-passing of the restrictions of frozen-shape nucleus-nucleus potentials. On the other hand more specific correlations of the fusion probability near threshold with nuclear deformability and static deformation,³⁻⁶ as well as with the presence of valence neutrons,⁷ have been reported.

In this Letter we present a comparative study of ^{40}Ar -induced fusion reactions using various Sn and Sm isotopes as targets. The measured fusion cross sections, which cover a range from several hundred millibarns down to the microbarn level, can be described by assuming the existence of a barrier fluctuation with an amplitude that is correlated with well-known collective surface properties of the nuclei.

Beams of ^{40}Ar varying from 3.2 to 4.5 MeV/u were provided by the UNILAC accelerator at the Gesellschaft für Schwerionenforschung, Darmstadt. Isotopically enriched targets of $^{112, 116, 122}\text{Sn}$ and $^{144, 148, 154}\text{Sm}$, 100 $\mu\text{g}/\text{cm}^2$ thick and on carbon backings of 40 $\mu\text{g}/\text{cm}^2$, were used. Except for ^{122}Sn (1.3% ^{124}Sn) and ^{154}Sm (97.7%), all targets had isotopic impurities of about 0.1%.

Two methods were applied to measure the evaporation residue cross sections. In method A, evaporation residues emitted in a forward cone of $\pm 1.5^\circ$ were separated from the projectile beam and other reaction products by the velocity filter SHIP⁸ and were mass analyzed with use of time-of-flight signals and energy signals from the implantation of the evaporation residues into a solid-state detector array. In method B the evaporation residues were stopped in thin Al catcher foils and the γ as well as the characteristic K x rays were counted in multiscaling mode over a period of several days.^{2,3} Catcher foils and x-ray activation were also used to determine the transmission through SHIP. By a comparison of the results from methods A and B, to be described elsewhere,⁹ a consistent set of cross sections with an estimated overall accuracy of 15% could be determined.

In the course of this work we have come to re-measure and revise some of the data in Ref. 3. In general the older data could be well reproduced, except for the $^{40}\text{Ar} + ^{154}\text{Sm}$ system where we found cross sections that were up to 30%

smaller for the higher energies. The difficulties in the earlier work probably resulted from unexpectedly large target inhomogeneities.

As in Ref. 4 we have measured fission cross sections with an ionization chamber. The fission decay branch, important for the Sm isotopes,⁴ was found to be less than 20% at the highest beam energies for the tin isotopes and rapidly decreasing with energy. More details will be given in Ref. 9.

Results for the total fusion cross sections are shown in Fig. 1. The data have been corrected for finite energy resolution; the energy scale is estimated to be accurate within 0.4 MeV. In Fig. 1 the ordinate and abscissa hold for the heavier of the Sm ($A=154$) and Sn ($A=122$) isotopes which are used as "references." For the lighter isotopes the following reduced fusion cross sections have been plotted:

$$\sigma^{\text{red}}(E) = (R_{B0}^2/R_B^2)\sigma(EV_{B0}/V_B),$$

where V_B and R_B are the barrier height and radius, respectively, calculated using the proximity potential,¹⁰ and the index zero indicates the reference isotope. The central radii to be used in the potential of Ref. 10 were calculated according to a droplet-model procedure¹¹ which reproduces rather well measured global isotopic trends in nuclear radii. This reasonably model-independent reduction serves to eliminate expected

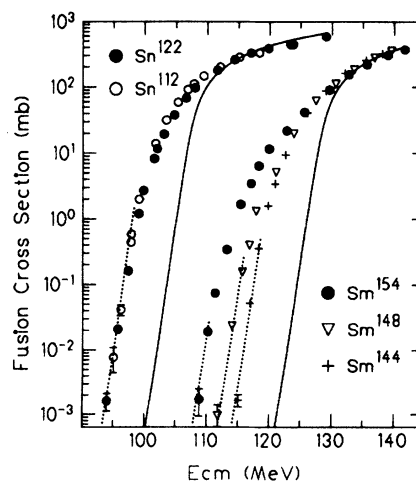


FIG. 1. Fusion excitation functions for the systems $^{40}\text{Ar} + ^{112, 122}\text{Sn}$, $^{144, 148, 154}\text{Sm}$. The ordinate and abscissa for the systems $^{40}\text{Ar} + ^{112}\text{Sn}$, $^{144, 148}\text{Sm}$ have been reduced as explained in the text. The full curves are conventionally calculated fusion excitation functions with a nuclear potential fitted in the energy range above the average fusion barrier.

“macroscopic” differences in the nucleus-nucleus potentials at the barrier due to the general increase of nuclear radii with mass. Use of other potentials discussed in Ref. 1 resulted in *relative* shifts of typically 0.2 MeV.

The cross-section “enhancement” is illustrated by comparison with a conventional barrier-penetration calculation (full curves) for the reference isotopes using an adjusted potential (see below). All excitation functions have two features in common: They tend to merge above the 200-mb level, and they have at sufficiently low energies approximately the same “universal” slope. The dotted lines in Fig. 1 have the same slope as the calculation and are simply displaced by a fixed energy relative to the full curves. In the following we shall discuss this displacement, which is constant for the Sn isotopes, but varies for the Sm isotopes, in terms of an effective potential model that includes a *fluctuation* of the fusion barrier with an amplitude that will be shown to be correlated with the collective surface properties of the partially excited nuclei. This model allows a description of the fusion excitation function over the entire measured energy range in terms of two parameters only, the average barrier V_B and its standard deviation $\sigma(V_B)$.

More explicitly, the effective nuclear potential

used was of the simple radial form^{10,12}

$$V(s) = V_n R_{12} \exp(-s/d) \quad (1)$$

with $s = r - (R_1 + R_2)$ and $R_{12} = R_1 R_2 / (R_1 + R_2)$. The average values of the central radii R_1, R_2 were deduced from published rms radii reduced¹¹ by the influence of the finite “skin” thickness and the static deformation (for ^{154}Sm). The diffuseness d was fixed at 0.75 fm.¹⁰ The barrier penetration was calculated with the WKB method. The known static deformation of ^{154}Sm was taken into account by generalizing Eq. (1) to ellipsoidal shapes and averaging the cross sections over all orientations of the symmetry axis relative to the beam axis.⁴ The Coulomb potential included monopole and quadrupole terms. For any set of parameters $V_n, R_1 + R_2$, and d the value of the barrier can be obtained by simply using Eq. (1). In particular, to an assumed Gaussian distribution of the sum of radii with a standard deviation $\sigma(R_1 + R_2)$ around its average value (not including the contributions from orientational fluctuation), there will be a corresponding distribution $\sigma(V_B)$ of the barrier heights and the resulting excitation function will be obtained by a weighted superposition. The data were least-squares fitted by adjusting V_n and $\sigma(R_1 + R_2)$. As examples, Fig. 2 shows for a “spherical” (^{122}Sn) and for a statically deformed (^{154}Sm) target nucleus the results of such two-parameter fits (full curves) to the data. The measured cross sections are well described over the available 5.5 orders of magnitude.

The parameter values, summarized in Table I, include results from fits of similar quality to the $^{16}\text{O} + ^{148}, ^{154}\text{Sm}$ data of Ref. 3, and were found to be insensitive to (a) a modification of d by 20%

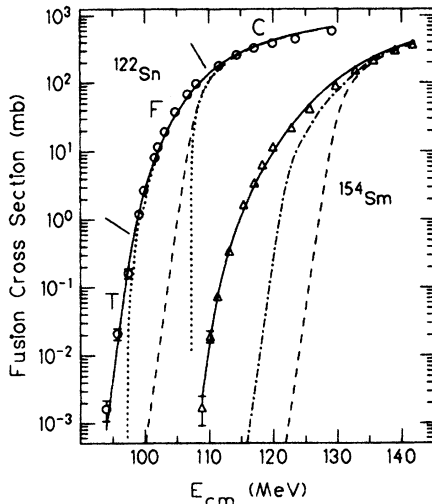


FIG. 2. Various calculations for the systems $^{40}\text{Ar} + ^{122}\text{Sn}$ and $^{40}\text{Ar} + ^{154}\text{Sm}$ made in an effort to parametrize and interpret the measured (symbols) fusion excitation functions. The full curves are two-parameter fits to the data, the dashed curves are calculations with the same nuclear potential, but without barrier fluctuation and static deformation. The other curves are explained in the text.

TABLE I. Barriers $V_B (\pm 0.5 \text{ MeV})$ and their relative standard fluctuation $\sigma(V_B)$ deduced from the fusion data. The corresponding surface-to-surface fluctuations $\sigma(R_1 + R_2)$ are compared to the fluctuations σ_{zp} expected from vibrational zero-point motion.

System	V_B (MeV)	$\sigma(V_B)$ (%)	$\sigma(R_1 + R_2)$ (%)	$\sigma_{zp}(R_1 + R_2)$ (%)
$^{40}\text{Ar} + ^{112}\text{Sn}$	109.1	4.0	4.7	4.85
$^{40}\text{Ar} + ^{116}\text{Sn}$	108.3	3.9	4.6	4.95
$^{40}\text{Ar} + ^{122}\text{Sn}$	107.2	3.9	4.5	4.85
$^{40}\text{Ar} + ^{144}\text{Sm}$	130.2	3.4	3.9	4.4
$^{40}\text{Ar} + ^{148}\text{Sm}$	129.4	4.3	4.9	5.0
$^{40}\text{Ar} + ^{154}\text{Sm}$	129.3	3.75	4.2	3.8
$^{16}\text{O} + ^{148}\text{Sm}$	60.25	2.9	3.6	4.5
$^{16}\text{O} + ^{154}\text{Sm}$	59.9	2.2	2.8	2.3

(with readjusted V_n) and (b) a replacement of the "radii fluctuation" by a "diffuseness fluctuation," showing that the origin of the barrier fluctuation need not be fully understood to deduce it experimentally.

In Fig. 2 we illustrate for the ^{122}Sn target how the introduction of a barrier fluctuation phenomenon influences the general behavior of the excitation function. If we first shut off the tunneling process in the calculation, we obtain the left-hand dotted curve, which fails to describe the energy range marked "T" below the millibarn level, but describes well the range above it. Therefore, in our model, information on the "pure" barrier penetration process can only be obtained from the very-low-cross-section data in the range T. If we also shut off the fluctuations (right-hand dotted curve), we can still describe the data in the "classical" range marked "C". It can be further shown that in this classical range the data are totally insensitive not only to barrier penetration, but also to the assumed amplitude of the barrier fluctuation. The latter is determined rather well from the intermediate "fluctuation" range "F," once V_B (or equivalently in our model, V_n) has been fixed by the data in range C.

For ^{154}Sm we have also plotted a curve showing separately the effect of the "orientational" fluctuations, i.e., the static deformation (dash-dotted curve). The dashed curves represent the conventional calculation without static deformation and "vibrational" fluctuations. They are identical to the full curves in Fig. 1.

Following the ideas of Esbensen,¹³ "vibrational" fluctuations in V_B are due to the fluctuation of the surface-to-surface distance originating from the collective vibrational motion of the nuclear surfaces. In this case the quantity $\sigma(R_1 + R_2)$ should have a direct link to the collective vibrational model. In fact, the zero-point standard-fluctuation width $\sigma_{zp}(R)$ of the nuclear radius is simply related to the "isoscalar deformation length" βR determined in the analysis of inelastic scattering experiments by $\sigma(R) = \beta R / (4\pi)^{1/2}$, Refs. 12 and 13. Thus, for the estimate of the surface to surface fluctuations, deformation lengths were taken from (α, α') or (d, d') inelastic scattering studies when available, or else they were obtained from published $B(EL)$ values with the assumption of equal deformation lengths for the charge and mass distributions. Only quadrupole and octupole vibrational transitions to the ground state with energies less than 3 MeV were included, since a classical estimate of the time

spent in the vicinity of the barrier in a fusion reaction just above the barrier suggested that vibrational modes with energies of 6-7 MeV or more would be "averaged out." A check of the adiabatic cutoff frequency by future dynamic calculations will be interesting. Octupole and quadrupole vibrational modes were added incoherently.

The resulting relative standard zero-point vibrational fluctuations are included in the last column of Table I. They are consistent in detail with the values deduced from the fusion-barrier fluctuation, both having an estimated accuracy of about 10%. A closer inspection also shows that (1) among the Sm isotopes it is the transitional nucleus ^{148}Sm which has the largest fluctuation, and (2) the fluctuation is larger for ^{40}Ar - than for ^{16}O -induced fusion. The latter observation is at least in part connected with the availability of a low-lying 2^+ state (1.46 MeV) in ^{40}Ar , but not in ^{16}O . Further, one expects an increased vibrational excitation at the barrier in the reaction with the more massive projectile.

In conclusion, we suggest that the apparent "subbarrier enhancement" of fusion cross sections is due to a dynamic barrier fluctuation caused by orientational and vibrational fluctuations of the surface-to-surface distance at the barrier. The amplitude of this fluctuation is consistent with well-known deformation lengths deduced from collective-model analyses of data on inelastic heavy-ion scattering to low-lying quadrupole and octupole states. The resulting excellent reproduction of the fusion data shows that there is no need to invoke additional degrees of freedom such as neck formation.

¹L. C. Vaz, J. M. Alexander, and G. R. Satchler, Phys. Rep. **69**, 373 (1981).

²U. Jahnke *et al.*, Phys. Rev. Lett. **48**, 17 (1982).

³R. G. Stokstad *et al.*, Phys. Rev. Lett. **47**, 465 (1978).

⁴R. G. Stokstad *et al.*, Z. Phys. **295**, 269 (1980).

⁵W. Scobel *et al.*, Phys. Rev. C **11**, 1701 (1975).

⁶B. Sikora *et al.*, Phys. Rev. C **20**, 2219 (1979).

⁷M. Beckerman *et al.*, Phys. Rev. Lett. **45**, 1472 (1980), and Phys. Rev. C **23**, 1581 (1981), and **25**, 837 (1982).

⁸G. Münzenberg *et al.*, Nucl. Instrum. Methods **161**, 65 (1979).

⁹W. Reisdorf *et al.*, to be published.

¹⁰J. Blocki *et al.*, Ann. Phys. (N.Y.) **105**, 427 (1977).

¹¹W. D. Myers and K.-H. Schmidt, in Proceedings of

the International Conference on Nuclei Far from Stability, Helsingør, 1981, CERN Report No. 81-09, 1981 (unpublished), Vol. 1, p. 90.

¹²R. A. Broglia and A. Winther, *Heavy Ion Reactions* (Benjamin, London, 1981), Vol. 1.

¹³H. Esbensen, Nucl. Phys. **A352**, 147 (1981).

Z Dependence of Strongly Interacting Relativistic Nuclear Fragments

Malcolm H. Mac Gregor

Lawrence Livermore National Laboratory, Livermore, California 94550

(Received 12 March 1982; revised manuscript received 6 August 1982)

Three different experimental groups have recently published the results of their investigations on highly interacting relativistic nuclear fragments (denoted as "anomalons"). These results are combined to form an anomalon data base, and then χ^2 analyses are used to demonstrate that the anomalon mean free paths are Z dependent. It is also demonstrated that these anomalon mean free paths lie on the boundary that delineates the "domain of nuclear forces."

PACS numbers: 25.70.Bc, 21.10.Ft, 21.60.Gx

When relativistic nuclei are incident on emulsions, some projectile fragments are observed¹⁻³ that have anomalously short mean free paths, a factor of 5 or so shorter than the mean free paths (mfp's) for uncollided beam particles with the same energies and Z values. Furthermore, this anomalous behavior persists through successive cascade fragmentations in the emulsion, as a sort of "memory" effect.¹ These strongly interacting nuclear fragments are now denoted as "anomalons,"⁴ and they have been observed in statistically significant quantities in three recently reported experiments: two experiments performed at the Bevalac,^{1,2} and one high-altitude-balloon cosmic-ray experiment.³

The crucial question posed by these anomalon experiments is the following: Can the very short anomalon mfp's be accounted for by "conventional" nuclear physics, or must some new type of interaction be invoked? In order to answer this question, we must define the "domain" encompassed by conventional nuclear physics. We should also attempt to obtain all possible information about the Z dependence of the anomalon mfp's, since a nuclear physics explanation suggests a nuclear physics type of Z dependence, whereas a more radical explanation⁵ might involve a totally different Z dependence. The anomalon χ^2 analyses carried out to date^{1,2} have been based for simplicity on the assumption of a Z -independent anomalon mfp.

The Z -dependent mfp's for *uncollided* relativistic beam projectile nuclei (2 GeV/nucleon) are

customarily expressed¹ in terms of the equation

$$\lambda_b(Z) \simeq \Lambda Z^{-b}, \quad (1)$$

which is valid over the range $Z = 2 - 26$ where the approximation $A \simeq 2Z$ applies. Experimentally,¹⁻³ $\Lambda \simeq 25 - 32$ cm, and $b \simeq 0.34 - 0.44$. For geometric cross sections, we would have $b = \frac{2}{3}$ in Eq. (1). The smaller values for b that are obtained experimentally are indicative of "shadowing" or "transparency" effects⁶ in the projectile nucleon cluster. A completely unscreened collection of nucleons would correspond to the value $b = 1$. Thus we see that the slope parameter b in Eq. (1) functions empirically as a nuclear screening coefficient.

In analogy to Eq. (1), we parametrize the *anomalon* Z dependence as

$$\lambda(Z) = \lambda_0(2Z)^{-b} \simeq \lambda_0 A^{-b}, \quad (2)$$

where λ_0 and b are determined by means of χ^2 fits to the anomalon data base.

We can roughly define the domain of nuclear forces in the following manner. Asymptotically, the high-energy nucleon-nucleon cross section, σ_n , corresponds to a mfp in nuclear emulsions, λ_n , of 36 cm.⁷ Since the general effect of combining several nucleons together is a reduction in the average nucleon interaction cross section,⁶ a collection of A nucleons that operates under conventional nuclear forces will have an effective total interaction cross section

$$\sigma_t \leq A \sigma_n, \quad (3)$$